

# Cracks in metallic meteorites

E. HORNBOKEN, E. MINUTH

*Institut für Werkstoffe, Ruhr-Universität Bochum, 4630 Bochum, West Germany*

Cracks in four meteorites with different nickel and phosphorus contents were investigated by optical microscopy. There are two types of cracks, those formed at elevated temperatures,  $700 > T_1 > 300^\circ\text{C}$ , and those formed at low temperatures,  $T_2 < 300^\circ\text{C}$ . The former modify the microstructure of the meteorite by acting as additional nucleation sites for the  $\gamma \rightarrow \alpha$  transformation of phosphide precipitation. This can be used to estimate the temperature of crack formation. The low-temperature cracks show the typical features of brittle fracture of steel. In addition, fracture along  $\gamma$ - $\alpha$  phase boundaries is often observed. This type of brittleness disappears if  $\text{Fe}_3\text{P}$  precipitates at these interfaces as small particles. Large phosphide particles can fracture at elevated as well as at lower temperatures. If reheating effects can be excluded, it is likely that the high-temperature cracks have been formed by shockwaves during a collision in the asteroid belt. They provide an important source of information on this event, if it occurs in the temperature range in which the  $\gamma$ -phase is stable. The low-temperature cracks form at embrittled sites in the microstructure during final impact with the Earth.

## 1. Introduction

From the point of view of materials science meteorites offer an opportunity to investigate solid matter which has undergone extremely low cooling rates of about  $10^{-6}\text{ K year}^{-1}$ . As metallic meteorites are predominantly alloys of iron with more than 5% nickel [1], microstructural features begin to appear at temperatures below which the  $\gamma \rightarrow \alpha$  transformation of the Fe-Ni solid solution starts, i.e. at  $T < 750^\circ\text{C}$ . The structure and composition of the  $\alpha$ -phase (kamacite) [2, 3] and the transformation products (plessite) of the residual  $\gamma$ -phase (taenite) [4] have been used to determine cooling rates and to estimate the diameter of the parent bodies as 100–200 km. The third alloying element is phosphorus, the solubility of which is higher in  $\alpha$ - than in  $\gamma$ -iron. During cooling it precipitates as  $\text{Fe}_3\text{P}$  (schreibersite, rhabdite). This phosphide can form in the  $\gamma$ -phase if its concentration is high [5]. Usually  $\text{Fe}_3\text{P}$  forms at  $\alpha$ - $\gamma$  interfaces [5, 6], grain or twin boundaries, or at dislocations at lower temperatures [7].

There has been much recent interest in the mechanical treatment experienced by meteorites during impact with the Earth. Shock-induced dislocations, twins and martensitic transformation

have been reported. Precipitation of  $\text{Fe}_3\text{P}$  at twin boundaries, recrystallization and the bulky interface of the  $\alpha$ -phase indicate that an additional mechanical treatment must have occurred at elevated temperatures at which thermally activated processes are not yet frozen in. These features can be distinguished from those which are due to reheating. From some meteorites a temperature before impact on the Earth of  $500$ – $400^\circ\text{C}$  has been estimated for this event [7]. A systematic review of the evidence for hot working of the  $\gamma$ -phase has been given by Axon and Faulkner [8]. Recrystallization twinning and formation of the  $\alpha$ -phase at non-octahedral slip planes are examples of deformation-induced defects. They will modify the microstructure which forms subsequently, if they cannot anneal out before the start of the  $\gamma \rightarrow \alpha$  transformation.

Many meteorites contain cracks. Most of them form during the final impact and are favoured by a low temperature and especially by segregation of phosphorus to  $\alpha$ - $\gamma$  phase boundaries or  $\alpha$ -grain boundaries [6]. However, the other type of crack mentioned above must have formed earlier in outer space [9]. This paper is concerned with the distinction between these two types of cracks.

TABLE I Composition of the meteorites.  $T_1$  = temperature of crack formation in outer space (see Fig. 10)

Meteorite origin	P (%)	Ni (%)	$T_1$ (°C)	Catalogue number
Hex River	0.25	5	~ 500	Vienna collection 8496*
Wichita County Rittersgrün	0.2 ~ 0.2	6.8 > 7	> 700 -	Vienna collection* Göttingen collection No. 91†
Gibeon	0.04	7.9	-	Vienna collection*

\*Naturhistorisches Museum, Wien, Austria.

†Mineralogisches Museum der Universität Göttingen.

## 2. Experimental results

The meteorites included in this investigation are listed in Table I in order of decreasing phosphorus content. Light microscopy of unetched and etched specimens proved to be most useful in revealing the origin of the cracks. In addition to nital, other etching reagents were used in this investigation which are less common in the investigation of meteorites. Their advantages, the better distinction of important phases and the distinction of orientation differences of crystallites of the  $\alpha$ -phase, are listed in Table II. Transmission electron microscopy provided supplementary information on the nature of plastic deformation, especially if it had to be confirmed that no reheating after impact on the Earth had occurred [7].

### 2.1. Hex River meteorite

The composition of this meteorite results in a high temperature for the  $\gamma \rightarrow \alpha$  transformation, which is complete at about 500°C. Two types of cracks are found in this meteorite: transcrystalline ones through the  $\text{Fe}_3\text{P}$  particles, and ones along

the  $\alpha$ - $\text{Fe}_3\text{P}$  interface. There is clear evidence that fracture of  $\text{Fe}_3\text{P}$  must have occurred at low temperatures in Fig. 1a, but at elevated temperatures in Fig. 1b. (Table III lists the nomenclature used in the micrographs in this paper.) Additional evidence for high-temperature (500°C) impact deformation stems from  $\text{Fe}_3\text{P}$  precipitation at twin boundaries and recrystallization at twin intersections (Fig. 2).

### 2.2. Wichita County meteorite

This meteorite shows deviations from the normal  $\{111\}_\gamma$  habit which are characteristic of the Widmannstätten structure (Fig. 3). The approximate orientation of the  $\alpha$  crystals as related to three traces of normal kamacite lamellae is shown in Fig. 4. It is evident that they are thicker than the average and that they form on both sides of the cracks. They are especially large at the crack tips, where  $\text{Fe}_3\text{P}$  is found more frequently than elsewhere (Fig. 5). Some  $\alpha$ - $\alpha$  cracks, which were pointing towards a rim of the  $\gamma$ -phase, showed a peculiar phenomenon (Fig. 6): the  $\alpha$ -phase had "broken through" this rim of  $\gamma$ -phase and had grown in an irregular way. The association of this secondary  $\alpha$ -phase with the shape of the cracks is evident and corresponds to that observed for primary formation of the  $\alpha$ -phase in this meteorite (Fig. 3). [A schematic drawing (Fig. 11b) to aid the discussion of the origin of this microstructural feature is included in Section 3.]

There was no evidence for the formation of non-Widmannstätten  $\alpha$ -phase at non-metallic inclusions in the  $\gamma$ -phase. It is possible that crack growth may continue during cooling of the meteorite into the temperature range in which  $\alpha$ -phase had formed. This growth may have been due to thermal fatigue. Different types of cracks form along the  $\alpha$ - $\gamma$  interfaces, as well as trans- and intergranular cracks in the  $\alpha$ -phase. These cracks are stopped by regions of  $\gamma$ -Fe-Ni and in

TABLE II Etchants used for microscopic examination of the meteorites.

Etching agent	Composition	Applications
1. Nital [10]	1 cm <sup>3</sup> HNO <sub>3</sub> , 100 cm <sup>3</sup> ethanol	Etching grain and phase boundaries
2. Alkaline sodium picrate [10]	25 g NaOH, 2 g picric acid, 75 cm <sup>3</sup> H <sub>2</sub> O	Blackening Fe <sub>3</sub> C
3. Klemm's reagent [11]	100 cm <sup>3</sup> saturated Na <sub>2</sub> S <sub>2</sub> O <sub>3</sub> , 6 g K <sub>2</sub> S <sub>2</sub> O <sub>5</sub>	Distinguishing between $\alpha$ - and $\gamma$ -Fe: $\alpha$ -Fe is covered with a coloured sulphide coat, $\gamma$ -Fe, Fe <sub>3</sub> C and Fe <sub>3</sub> P remain white

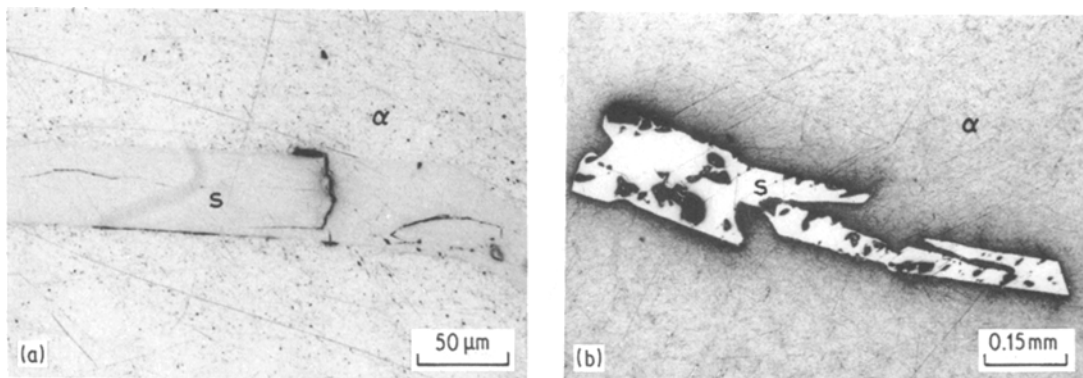


**Figure 1** Comparison of two types of cracks associated with  $\text{Fe}_3\text{P}$  particles in the Hex River meteorite. (a) Cracks in schreibersite ( $\text{Fe}_3\text{P}$ ) and at the  $\text{Fe}_3\text{P}$ - $\alpha$  interface, formed by brittle fracture during impact at low temperature ( $T_2$ ), unetched. (b) Cracked schreibersite ( $\text{Fe}_3\text{P}$ ) particle, showing plastic flow of the  $\alpha$  matrix between the fragments. The rounding-off of the corners indicates that the fracture has occurred at an elevated temperature,  $T_1 \approx 500^\circ \text{C}$ ; Etching agent 3.

the vicinity of  $\text{Fe}_3\text{P}$  particles (Fig. 7). There is evidence for shock-induced transformation in parts of this meteorite (Fig. 5b).

### 2.3. Rittersgrün meteorite

This meteorite has a typical non-Widmannstätten  $\alpha$ -phase which has nucleated along the rim of the interface formed with the ceramic environment of the metallic particles (Fig. 8a). Cracks form predominantly at  $\gamma$ - $\alpha$  interfaces (Fig. 8b). It is remarkable the cracks are never found if  $\text{Fe}_3\text{P}$  starts to nucleate at this interface (Fig. 8c).

### 2.4. Gibeon meteorite

In contrast to the Wichita County meteorite this meteorite shows exclusively the normal  $\{111\}_\gamma$  habit of the Widmannstätten structure (Fig. 9a). Precipitation of  $\text{Fe}_3\text{P}$  was neither expected nor found. This meteorite contains a number of cracks

formed at  $T_2$ , many of them being of the inter-crystalline  $\alpha$ - $\gamma$  and  $\alpha$ - $\alpha$  type (Fig. 9b). No  $T_1$  cracks were found in the investigated portions of the material.

## 3. Discussion

The cracks observed in these meteorites can be divided into two categories: those which have formed at a low temperature,  $T_2$ , and those which have effected the microstructure which develops during cooling. The latter must have formed at an elevated temperature  $T_1$ . This temperature can be estimated if the solid-state reactions which occur during cooling are known.  $T_2$  is the temperature of the meteorite when

TABLE III Symbols used to explain the micrographs

Symbols	Meaning*	Structural characteristics
$\alpha$	Kamacite	$\alpha$ -Fe-Ni, solid solution
$\alpha_c$	Kamacite, crack-induced	
$\gamma$	Taenite	$\gamma$ -Fe-Ni, solid solution
s	Schreibersite, Rhabdite	$\text{Fe}_3\text{P}$
p	Plessite	$\alpha + \gamma$ phase formed by transformation and decomposition of $\gamma$ phase
n	Neumann bands	$\{112\}$ deformation twins
r	Recrystallized crystals	

\*Or mineralogical name.

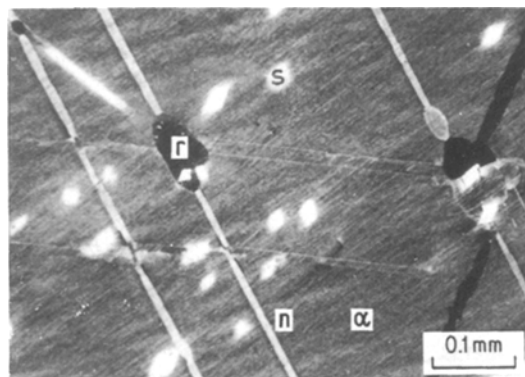


**Figure 2** Recrystallization at twin intersections provides further evidence for  $T_1$  deformation in the Hex River meteorite. These twins exist in addition to those which must have formed later on during final impact, i.e.,  $T_2$  twins. Etching agent 3; only kamacite is covered with a sulphide coating due to the orientation of the crystals.

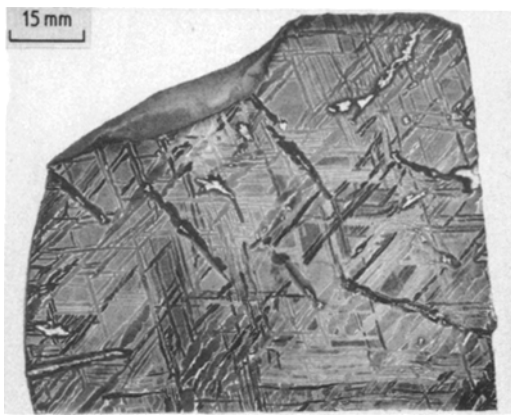


Figure 3 Survey of the Wichita County meteorite showing Widmannstätten kamacite and crack-nucleated non-Widmannstätten kamacite ( $\alpha$ -Fe); Etching agent 3.

hitting the Earth. Effects due to reheating after collision with the Earth can be excluded in all cases because such heat treatments would also have modified the defects produced by the final impact. Before this event, thermal cycling cannot be excluded. However, all the microstructural features can be explained consistently by continuous cooling from the temperature range in which the  $\gamma$ -phase is stable.  $T_1$  must be ascribed to an event in outer space. This is probably a collision in the asteroid belt (between Mars and Jupiter), which has produced fragments with new orbits which cross that of the Earth (Fig. 10). The question arises as to whether information additional to that obtained from the analysis of the morphology and composition of the crystalline phases can be expected from these cracks.

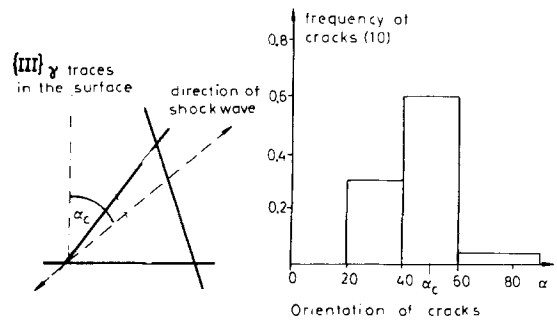


Figure 4 Analysis of crack traces in Wichita County meteorite to derive the most probable direction of a shockwave which may have passed the former taenite ( $\gamma$ -Fe) single crystal at  $T_1$ .

### 3.1. $T_1$ cracks

$T_1$  cracks are found in the structure of the Wichita County meteorite. Above about  $750^\circ\text{C}$  this had been a stable  $\gamma$ -single crystal. As nucleation of the  $\alpha$ -phase is associated with a high activation energy, nucleation is limited to the surface, non-coherent interfaces [6] and grain boundaries or dislocation groupings in slip planes [8], even after considerable undercooling. Fig. 3 provides evidence that additional nucleation sites had existed inside this crystal in the form of cracks. The  $\alpha$ -phase formed as a rim along the crack surface. The crack tips seem to have nucleated  $\alpha$ -crystals, in a similar manner to the nucleation of this structure at non-metallic inclusions [6, 7] (Fig. 8). These crack-nucleated  $\alpha$ -crystals had interacted with the normal Widmannstätten structure which had grown from other nucleation sites.

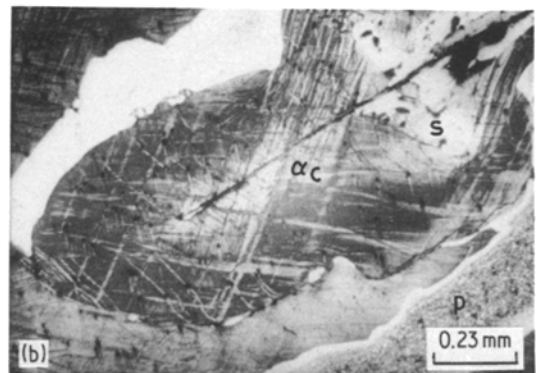
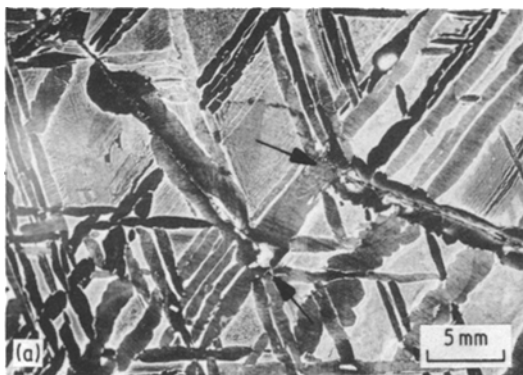
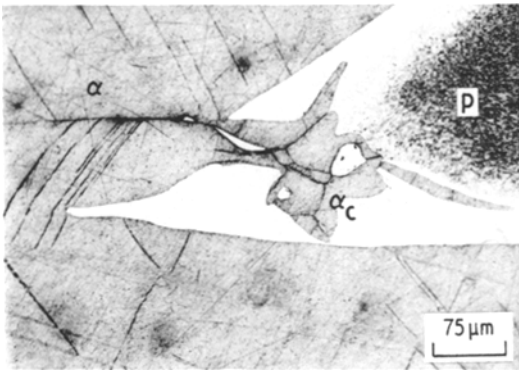
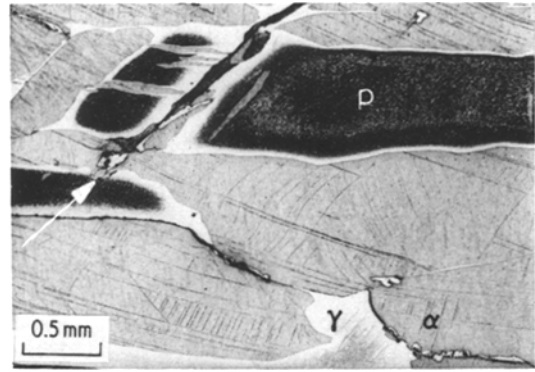


Figure 5 (a) Nucleation of kamacite ( $\alpha$ -Fe) and schreibersite ( $\text{Fe}_3\text{P}$ ) at crack tips (arrow) and crack surfaces in Wichita County meteorite; Etching agent 3. (b) Preferred nucleation and growth of kamacite ( $\alpha$ -Fe) at a crack tip; Etching agent 3.



**Figure 6** Nucleation of kamacite ( $\alpha$ -Fe) in Wichita County meteorite at a crack tip which has "broken through" a taenite ( $\gamma$ -Fe) rim; Etching agent 3.

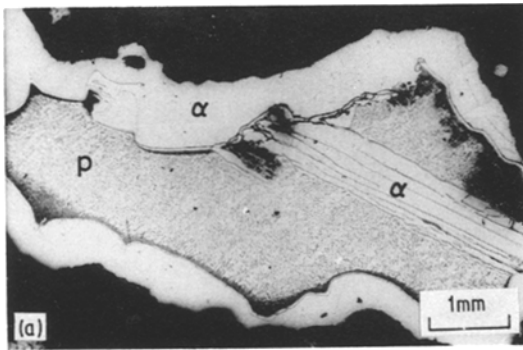
This interpretation implies that the cracks had existed in the  $\gamma$ -crystal before it entered into the  $\alpha + \gamma$  phase field, or at least in the possible range of undercooling, about  $100^\circ\text{C}$  below the equilibrium temperature  $T_{\gamma\alpha}$ :  $T_1 > 750^\circ\text{C}$ . Thus, an analysis of the cracks provides information on events which have occurred at temperatures  $T_1$  above those which can be probed by transformation and precipitation reactions:  $T_M > T_1 > T_{\gamma\alpha}$  ( $T_M$  is the melting temperature). The cracks in the tough  $\gamma$ -crystal showed no relation to its crystal-



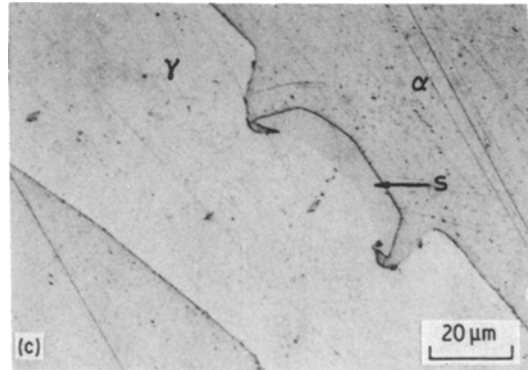
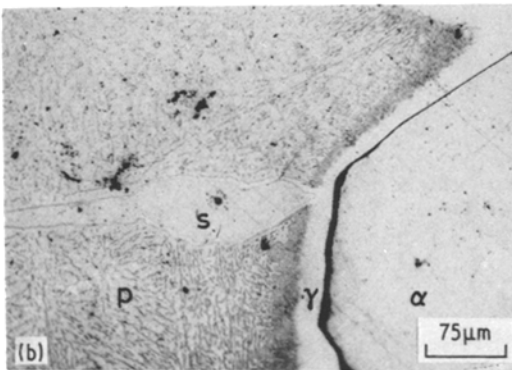
**Figure 7** Crack in Wichita County meteorite which has been stopped by a taenite ( $\gamma$ -Fe) rim at  $T_1$  (arrow) and consequently kamacite ( $\alpha$ -Fe), and schreibersite ( $\text{Fe}_3\text{P}$ ) at its tip and flanks. In addition, cracks at the  $\alpha$ - $\alpha$  and  $\alpha$ - $\gamma$  boundaries can be seen; these have formed at low temperature  $T_2$ ; Etching agent 3.

lographic planes but there was a preferred orientation in which they occurred most frequently (Fig. 4). All the characteristics of these cracks agree with the phenomenon of spalling, which is observed if compressive shockwaves are reflected by free surfaces. At a certain distance from the surface they create a maximum tensile stress. The fracture stress of a material can be surpassed easily at this site [12]. In bodies with irregular shapes these tensile stresses can be further amplified by interference of different waves.

Other  $T_1$  cracks were found in the Wichita



**Figure 8** Rittersgrün meteorite. (a) Rim-like, non-Widmannstätten kamacite ( $\alpha$ -Fe) which has formed by nucleation at the interface of a metallic particle embedded in the non-metallic matrix; Etching agent 1. (b)  $\alpha$ - $\gamma$  interfacial cracks which form at low temperature  $T_2$  as long as there is no nucleation of schreibersite ( $\text{Fe}_3\text{P}$ ) particles at this boundary to remove brittleness by segregation; Etching agent 2. (c) Uncracked  $\alpha$ - $\gamma$  interface with schreibersite ( $\text{Fe}_3\text{P}$ ) particle; unetched.



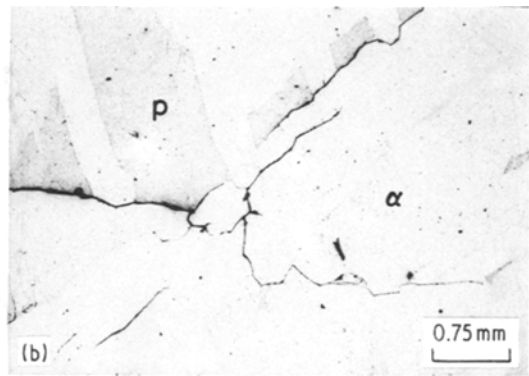


**Figure 9** (a) Survey of Gibson meteorite showing exclusively Widmannstätten kamacite ( $\alpha$ -Fe) (cf. Fig. 3); Etching agent 3. (b)  $\alpha$ - $\alpha$  and  $\alpha$ - $\gamma$  cracks which must have formed at low temperature  $T_2$ . There is no evidence for  $T_1$  cracking in the investigated part of this meteorite; unetched.

County meteorite; these must have formed or grown after the formation of the  $\alpha$ -phase had started (Fig. 6). The  $\alpha$ -lamellae were modified in areas where the crack could provide new sites for the nucleation of the more stable phase, mostly  $\alpha$ -phase occasionally  $\text{Fe}_3\text{P}$ . The Fe-Ni phase diagram [3] indicates that below  $600^\circ\text{C}$  only small changes in the volume ratio of the phases occur. Therefore the secondary  $T_1$  cracks in the Wichita County meteorite must have formed at  $600 > T_1 > 300^\circ\text{C}$ . At lower temperatures diffusional rearrangements become so slow that they cannot produce microstructural changes visible by optical microscopy. It is likely that subcritical crack growth has followed the critical formation of the primary crack caused by the shock wave. The cyclic load could have originated from thermal cycling. The Hex River meteorite contained evidence for  $T_1$  cracking only, in the form of shattered phosphide particles which can only have formed in connection

with the complete  $\gamma \rightarrow \alpha$  transformation (Fig. 1). This limits the temperature at which the first impact occurred to  $680 > T_1 > 300^\circ\text{C}$ . The formation of  $T_1$  cracks and its consequences are shown schematically in Fig. 11.

### 3.2. $T_2$ cracks

There is no doubt about the fact that these cracks originate from collision with the Earth. Most of the phenomena are well known from the brittle fracture of steels, e.g. the intercrystalline and transcrystalline fracture of the  $\alpha$ -phase. The extreme brittleness of the  $\alpha$ - $\gamma$  interface is typical for meteorites (Figs 7 and 12). This is observed if the  $\alpha$ -phase forms before the precipitation of  $\text{Fe}_3\text{P}$  starts, i.e., especially in high nickel, low phosphorus alloys. Cooling very slowly to low temperatures provides optimum conditions for saturation of phosphorus segregation to these sites. This element is redistributed as soon as the  $\alpha$ -phase starts to form. Its solubility is higher in the bcc lattice and consequently phosphorus atoms diffuse in a direction opposite to that of the motion of the  $\gamma$ - $\alpha$  interface (Fig. 12). If  $\text{Fe}_3\text{P}$  has nucleated the conditions for de-segregation are equally favourable in meteorites. As the solubility at ambient temperature is negligible, all phosphorus should be concentrated inside the particles [13, 14]. This agrees with the observation that  $\gamma$ - $\alpha$  interfacial brittleness disappears immediately, even if rather widely spaced  $\text{Fe}_3\text{P}$  particles appear. Only very large phosphide particles and their interface can become additional sites for crack nucleation.

Cracks can provide additional information on

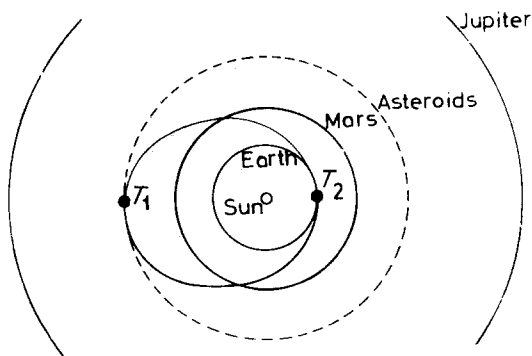


**Figure 10** Hypothetical history of meteorites; collision in the asteroid belt at  $T_1$ , followed by impact on the Earth at  $T_2$ .

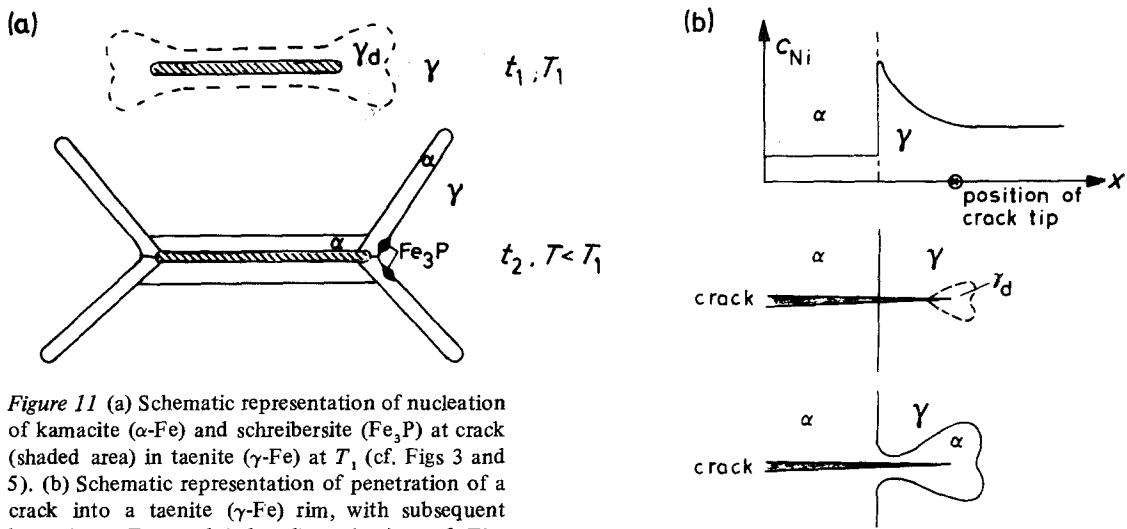


Figure 11 (a) Schematic representation of nucleation of kamacite ( $\alpha$ -Fe) and schreibersite ( $\text{Fe}_3\text{P}$ ) at crack (shaded area) in taenite ( $\gamma$ -Fe) at  $T_1$  (cf. Figs 3 and 5). (b) Schematic representation of penetration of a crack into a taenite ( $\gamma$ -Fe) rim, with subsequent kamacite ( $\alpha$ -Fe, crack-induced) nucleation (cf. Figs 6 and 7).  $\gamma_d$  = deformed taenite ( $\gamma$ -Fe) at crack tip, which provides nucleation sites for kamacite ( $\alpha$ -Fe).

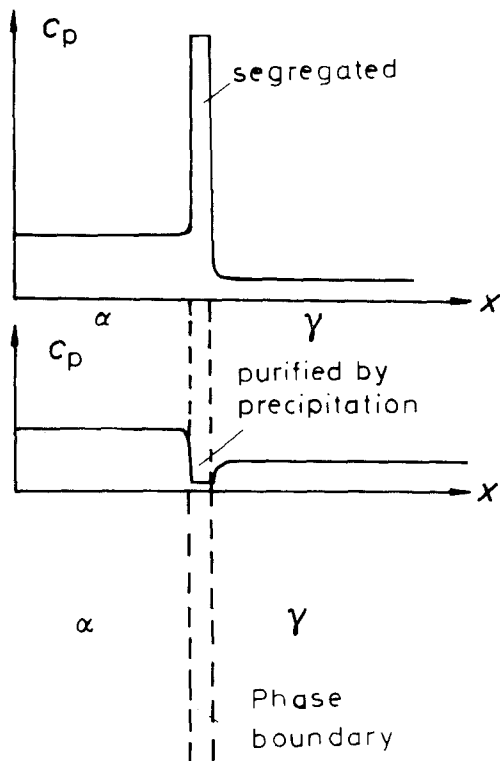


Figure 12 The origin of brittleness of the  $\alpha$ - $\gamma$  interfaces is phosphorus segregation (cf. Figs 7, 8b and 9b). It is avoided by precipitation of schreibersite ( $\text{Fe}_3\text{P}$ ) at these boundaries. As long as no nucleation of phosphide particles has started, the phosphorus at these boundaries is highly segregated. Formation of  $\text{Fe}_3\text{P}$  particles will be connected with de-segregation at these boundaries.

the prehistory of meteorites and are the only source of information for the range of high temperatures in which no solid-state reactions take place and deformation-induced defects have annealed out. On the other hand, the study of meteorites can provide insight into mechanisms of intercrystalline embrittlement of iron alloys, because they provide examples for equilibrium segregation at various interfaces which cannot be obtained by any experimental heat treatments.

### Acknowledgements

The meteorites used in this investigation came from collections at the Universität Göttingen and the Naturhistorisches Museum, Wien. We are indebted to Dr G. Kurat for his help in selecting cracked meteorites from the Vienna collection.

### References

1. V. F. BUCHWALD, *Phil. Trans. Roy. Soc. A* 286 (1977) 453.
2. J. I. GOLDSTEIN, *Geochim. Cosmochim. Acta* 31 (1969) 1733.
3. J. I. GOLDSTEIN and H. J. AXON, *Naturwiss.* 60 (1973) 313.
4. T. B. MASSALSKI, F. R. PARK and L. F. VASSAMILET, *Geochim. Cosmochim. Acta* 30 (1966) 649.
5. A. S. DOAN, JR and J. I. GOLDSTEIN, in "Meteorite Research" edited by P. M. Millman (Reidel, Dordrecht, Holland, 1969) pp. 763-99.
6. K. ABRAHAM and E. HORNBOKEN, *Z. Metallkunde* 65 (1974) 712.
7. E. HORNBOKEN and H. KREYE, *ibid* 61 (1970) 914.
8. H. J. AXON and D. FAULKNER, *Geochim. Cosmochim. Acta* 31 (1967) 1539.
9. V. F. BUCHWALD, "Handbook of Iron Meteorites",

- (University of California Press, Berkeley USA, 1975).
10. "Metals Handbook", Vol. 8 edited by T. Lyman (American Society for Metals, Metals Park, Ohio, 1973) p. 91.
  11. M. BECKERT and H. KLEMM, "Handbuch der Metallografischen Akverfahren", (VEB, Leipzig, 1966) pp. 61-4.
  12. J. L. O'BRIEN and R. S. DAVIS, in "Response of Metals to High Velocity Deformation" edited by P. C. Shewman and V. F. Zackay (Interscience, New York, 1961) pp. 371-88.
  13. E. HORNBOKEN, *Trans. ASM* 53 (1961) 569.
  14. *Idem, ibid.* 55 (1967) 719.

Received 20 March and accepted 4 August 1980.